Trichroic Vibrational Analysis on the α-Form of Poly(lactic acid) Crystals Using Highly Oriented Fibers and Spherulites

Kaoru Aou and Shaw Ling Hsu*

Department of Polymer Science and Engineering and Materials Research Science and Engineering Center, University of Massachusetts, Amherst, Massachusetts 01003

Received September 21, 2005; Revised Manuscript Received January 19, 2006

ABSTRACT: Infrared and Raman spectra of the PLA α-crystal were analyzed. Detailed analysis is only possible by using highly oriented electrospun fiber mat. Infrared dichroic analysis of large two-dimensional PLA crystals was also conducted. By combining the two dichroic analyses, accurate band assignments for an α-crystal were achieved for the first time. This analysis is only consistent with a 10/3 helical chain conformation, as opposed to the more simplistic 3/1 helix generally used. Infrared and Raman activities of the PLA 10/3 single-chain helix were derived and correlated to the orthorhombic α-crystal. The orthorhombic structure, previously suggested from X-ray studies, was confirmed by vibrational analysis. Poorly understood spectral features, such as the unexpectedly large number of carbonyl stretching vibrations, are attributed to crystal field splitting. An additional Raman component has its origin due to Fermi resonance interactions.

Introduction

Poly(lactic acid), or PLA, is one of the few commercially viable biomass-derived polymers. PLA is derived from sustainable and renewable resources, as its L- and D-lactic acid monomers themselves are derived from saccharides through fermentation.[1] Since 2002, fibers and films composed entirely of this biopolymer have been commercially available in large volume. Systematic incorporation of D-lactyl moieties in the PLA backbone can significantly alter physical properties, morphology, and morphological development, such as crystallization,[2] orientation,[3] or physical aging.[4,5] As it is biodegradable, PLA has been incorporated in medical applications.[6,7] Other applications in nanopatterning have recently been proposed.[8]

Because of uncertain structures, understanding processing-induced structural changes, e.g. segmental orientation or crystallite size in PLA, was difficult to achieve.[9−11] Analysis of PLA diffraction data was also difficult. The space group of the PLA α-crystal has been unambiguously assigned as $P2_12_12_1$, but actual atomic coordinates as well as the helical symmetry associated with PLA α-crystals have been in dispute.[12,13] In Figure 1, two proposed structures from the literature are shown schematically. The particular advantages of vibrational spectroscopy have been utilized to probe crystallization behavior[14] and to follow conformational changes due to deformation processing.[11]

A large number of vibrations remain unexplained. No clear explanation was available for the rich features observed in the carbonyl stretch region (from 1700 to 1850 cm^{-1}). This vibration is an extremely localized motion. Multiple components are not expected since the carbonyl units are localized. While helical symmetry was speculated as the cause for the multiple bands in this frequency region,[15] no evidence was provided to support this assignment. Raman-active bands were erroneously assigned to four symmetry species, including the optically inactive B species. This is inconsistent with the well-established fact that helical groups have only three optically active vibrational symmetry species corresponding to phase angles of 0, ψ, and 2ψ, where ψ is the helical angular rotation per residue.[16] In the three references treating PLA as a C_{10} line group, two assign incorrect vibrational activity to a symmetry species[15,17] and the third has some typographical errors in the character table itself.[18] An accurate C_{10} character table necessary for vibrational analysis has heretofore not been available.

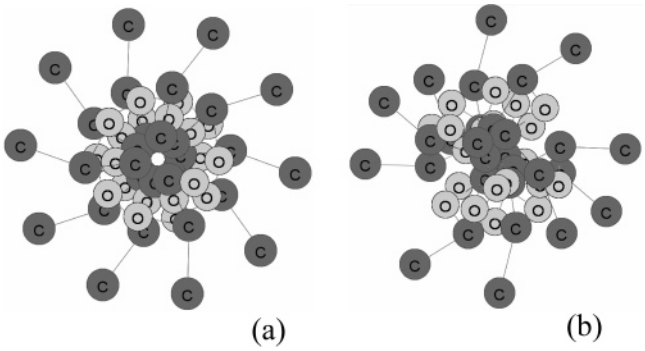

Figure 1. Two proposed forms of the α-crystals: (a) Aleman/Puiggali/Lotz coordinates; (b) Sasaki/Asakura coordinates. Hydrogens are abbreviated to aid clarity.

Proper assignment of molecular vibrations is of fundamental importance specifically when morphological studies are conducted through vibrational spectroscopy, such as crystal orientation[10] or amorphous deformation.[11] Whether a spectral change is caused by a peak shift or simultaneous intensity changes in two or more separate bands determines the accuracy of the molecular interpretation of spectral data and can be determined only when proper normal mode assignments are established.

Vibrational spectroscopy has been used to analyze molecular order and orientation in both crystalline and amorphous features in PLA.[9,11,19,20] Without achieving proper orientation distribution, desired properties such as mechanical strength or dimensional stability cannot be attained.[20] To assign fundamental vibrational modes that have dipole derivative vectors coincident with the three crystallographic directions of polymer crystals, it is necessary to have a sample or samples where orientation in two of the three crystallographic axes is achieved. This ordinarily meant having a large and thin single crystal in the case of infrared absorption spectroscopy. In practice, one employs the single-chain approximation, i.e., intermolecular interactions are neglected,[21] to assign vibrational features. Refinements may be achieved by taking intermolecular interactions into account. For example, this was conducted to explain the experimentally observed band splitting associated with the orthorhombic form of crystalline polyethylene.[22,23] The single-chain model would assume some helical structure for the polymer, determined most commonly using X-ray diffraction

10.1021/ma052058+ CCC: $33.50
Published on Web 03/30/2006

on oriented polymer samples as well as using molecular modeling. This method allows for the unambiguous determination of vibrations with components in the *c*-axis (by convention, this is defined as the helical direction and fiber axis for all polymeric crystals), which coincides with the orientation direction for 100% uniaxially oriented samples. The vibrations with components in the *a*- and *b*-axes are, however, not distinguishable through this method as the two axes perpendicular to the *c*-axis are indistinguishable in uniaxially oriented samples. Splittings between vibrations associated with the *a*- and *b*-axis would therefore require the extension of vibrational analysis from the helical chain structure to the entire crystal unit cell.

Previous infrared analysis performed on oriented PLA used the attenuated total reflectance (ATR) technique, since the available oriented films were too thick for transmission experiments. Although ATR-infrared data have been obtained in the past, there is still considerable value in conducting an infrared study on oriented PLA materials in the transmission mode as opposed to ATR because in ATR small shifts in frequency and relative intensity are hard to predict. Vibrational assignments were previously based on a normal-coordinate analysis of a PLA single chain 3/1 helix combined with polarized infrared and Raman spectroscopic analysis.[24] It was recently found that the crystallographic *a*-axis of the α-form has exclusive orientation in the direction of the spherulitic radius.[25] This fact, combined with standard infrared dichroism analysis on a drawn and annealed PLA film, enables a trichroic vibrational analysis not requiring the preparation of a large and thin single-crystal necessary for a transmission infrared experiment which is difficult to prepare.

Unambiguous assignments of α-crystal vibrational frequencies (infrared and Raman) are of great value. However, some uncertainties exist with PLA structures making vibrational assignments less than definite. Under ordinary conditions, the α-form is the only one obtained.[13,26] Four rotational isomeric states are generally used to describe an idealistic helix. These are *tg′t*, *tg′g*, *ttt*, and *ttg*, existing in 80%, 10%, 5%, and 5%,[27] where the notation *tg′t* refers to a trans planar ester C−O, gauche O−C_α, and trans C_α−C torsions, respectively. Only relatively extreme conditions, such as spinning an α-crystalline fiber[28] or extruding an α-crystalline billet in the solid state,[29] can produce a *β*-crystal. Stereocomplex crystals of PLA can form in the presence of a 1:1 mixture of L-rich and D-rich PLA material.[30,31] A fourth form, the *γ*-form, is reported to form epitaxially under appropriate conditions.[31] These are the four known crystal polymorphs to PLLA. In this study, two particularly well-defined samples were used. First, highly oriented filmlike mats of electrospun fibers were obtained. In addition, exceptionally large 2-D spherulites with diameters of about 5 mm were prepared. Both samples are in the α-crystalline form and are sufficiently large and thin to produce highly polarized infrared spectra.

Under practical circumstances, only the α-crystal is obtained. We therefore focused on analysis of vibrational spectra obtained using this structure. The $P2_12_12_1$ space group of the α-crystal has D_2 group symmetry, the character table of which is well-known, and has four symmetry species: A, B_1, B_2, and B_3.[32] Only the B_1, B_2, and B_3 species are infrared-active, with dipole derivative vector components in the *c*-, *b*-, and *a*-directions or equally *z*-, *y*-, and *x*-directions, respectively. All four symmetry species are Raman-active, where the A species are polarized and the other three depolarized. Knowledge of these optical activities combined with appropriate polarized spectroscopy permits trichroic analysis on the spherulite and the oriented fiber mat polarized infrared spectra. Results are presented here.

Materials and Experimental Techniques

Samples of poly(L-lactic acid), or PLLA, of 1.2% D-lactyl content were received from NatureWorks LLC and used for our PLA α-crystal studies. Chloroform, a good solvent for PLA, was used as received from Sigma-Aldrich. *N*,*N*-Dimethylformamide (DMF) from Fisher Scientific was used as received. Because of its high boiling point and polarity, DMF was used as a cosolvent to suppress the rapid evaporation of chloroform and assist the electrospinning process.

For observing crystal orientation in the spherulite, a Rigaku X-ray generator with an in-house built Statton camera was used to obtain an X-ray diffraction pattern. The sample was mounted in front of the 200 μm Statton camera pinhole. 40 kV and 30 mA were maintained throughout exposure for 1 h. An image plate was used to record diffraction intensity.

Highly oriented mats of PLA were prepared using previously published electrospinning techniques and were used to obtain polarized transmission infrared spectra.[33] The solution concentration was 9.4 wt % PLLA. DMF and chloroform in 1:3.8 ratio by weight was used as the electrospinning solvent medium. The PLLA/chloroform solution was prepared first and solubilized with gentle stirring overnight, followed by addition of DMF. The solution flow rate used during electrospinning was 0.020 mL/min at the syringe end. A potential of 14 kV was applied from the syringe tip to the grounded rotating target. Further orientation was applied using a manual tensile stretcher at 120 °C then annealed at that temperature for 5 min. The oriented sample was sufficiently thin for use in transmission experiments. Because of the fact that well-separated parallel and perpendicular bands are observed in the polarized infrared spectra, the orientation in the sample was sufficient for our studies on the assignment of vibrational species to observed frequencies.

Spherulitic samples were prepared from cast films of PLLA from a solution of chloroform. The films were always dried under vacuum for at least an hour. The absence of residual solvent was confirmed for each sample using the infrared absorption peak for chloroform at 668 cm^{-1}. Samples were cooled to crystallization temperature directly from the melt (220 °C for 1 min) to obtain two-dimensional (2D) spherulites. Alternatively, samples could first be quenched from the melt to room temperature and then warmed to crystallization temperature to obtain three-dimensional (3D) spherulites.

Infrared spectra for PLA at liquid nitrogen temperature were acquired using a Bruker IFS-113v vacuum FT-IR spectrometer and a custom-built cold cell. Spectral resolution was maintained at 1 cm^{-1}. Zinc selenide plates were used in all infrared studies, since they were the only material with a wide frequency range of transparency that could also withstand substantial thermal shock such as quenching from the melt to room temperature. Polarized infrared spectra were obtained using a Perkin-Elmer Spectrum 2000 FT-IR spectrometer with a wire grid polarizer to apply linear polarization to the incident infrared beam. Resolution was maintained at 4 cm^{-1} in order to achieve an acceptable signal-to-noise ratio. All infrared spectra in this study have been obtained using the transmission technique.

A Jobin-Yvon Horiba LabRam HR800 dispersive Raman spectrometer was used to obtain polarized and depolarized Raman spectra. The 632.8 nm line of the helium−neon gas laser was used for excitation. Spectral resolution of less than 4 cm^{-1} was maintained near the laser line. The effectiveness of the polarization analyzer was confirmed using depolarized Raman bands of a carbon tetrachloride standard. As a testament to the effectiveness of the polarizer, the polarized band at 460 cm^{-1} showed a depolarization ratio of 0.01. In agreement with theory, depolarization ratios of 0.78 ± 0.03 were obtained for all depolarized bands.[32] Isotropic spectra were computed using the formula $I_{iso} = I_{||} - {}^4/_3 I_\perp$, where I_{iso}, $I_{||}$, and $I_\perp$ are the isotropic, polarized, and depolarized spectra, respectively.

The normal-coordinate analysis computer program, developed at the University of Michigan,[34] was used to compute normal frequencies of 3/1 and 10/3 single-chain helices. The atomic

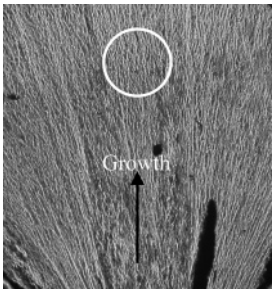

Figure 2. Spherulite observed under polarized optical microscopy. The approximate region probed by the X-ray is indicated by the circle. Center of the spherulite lies outside the photographed area. "Growth" indicates the radial growth direction.

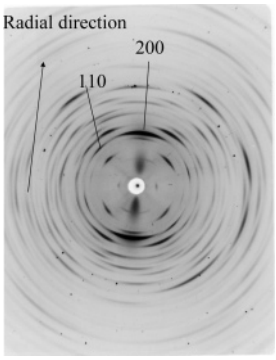

Figure 3. X-ray diffraction pattern of PLA 2D spherulite, along the radial direction.

coordinates used to calculate infrared and Raman features of a 10/3 α-helix frequency were transferred directly from a previous study,[13] as were those used to calculate the vibrational spectrum of a 3/1 helix.[31] The force constants are the same as in our previous work using our definition of internal coordinates and symmetry coordinates.[24] A character table for C_{10} (10/3 helix) was derived using the method prescribed by Wilson, and the character table for C_3 (3/1 helix) was taken directly from Wilson.[32]

To simulate the infrared absorbance of the carbonyl bands, dipole derivatives of the carbonyl stretching vibrations were estimated by running an ab initio vibrational calculation on a model compound using Gaussian98.[35] The basis set used was 6-31G(d), and a B3LYP density functional level of theory was employed. The geometry of the model compound, 2-methoxymethylpropanoate, was constrained so as to approximate real PLA helix conformations. As before, the ester C−O torsion was fixed at 180.0°, the O−C_α torsion at −73.0°, and the C_α−C torsion at 160.0°.[36]

Results and Discussion

The infrared-active 923 cm^{-1} band was used to confirm the presence of the α-form of PLA crystals.[20] A polarization study was carried out for a stretched PLA film. In a past study, because of sample thickness, the attenuated total reflectance (ATR) technique was used.[36] In the present study, a significantly thinner oriented PLA mat was obtained using the electrospinning technique. We were able to obtain polarized infrared spectra of exceptional signal-to-noise ratio using the transmission technique. The quality of polarized spectra in the current study is very high in terms of the signal-to-noise and dichroic ratios obtained. We also investigated 2D and 3D spherulites. In the case of 2D spherulites, X-ray diffraction results were used to demonstrate crystal orientation in the radial direction. The sample and spot location probed with X-ray diffraction is shown in Figure 2. The (200) reflection lies on the radial direction of the spherulite, as shown in Figure 3, indicating that the crystallographic *a*-axis is coincident with the spherulitic radial direction. The diffraction spots are also very small, indicating the high extent of crystal orientation. Combining polarized infrared absorption data of a uniaxially oriented film (*c*-axis oriented) and a 2D spherulite (*a*-axis oriented) enables in effect an infrared trichroic analysis on the PLA α-crystal.

Table 1. Character Table of the C_{10} Group[a]

C_{10} group	E	$2C_{10}^3$	$2C_5^2$	$2C_{10}$	$2C_5$	C_2	spectroscopic activities
A	1	1	1	1	1	1	T_z, $\alpha_{xx}+\alpha_{yy}$, α_{zz}
B	1	−1	1	−1	1	−1	inactive
E_1	2	$-\phi$	$-1-\phi$	$1+\phi$	ϕ	−2	(T_x, T_y), (α_{yz}, α_{zx})
E_2	2	$-1-\phi$	ϕ	ϕ	$-1-\phi$	2	($\alpha_{xx}-\alpha_{yy}$, α_{xy})
E_3	2	$1+\phi$	ϕ	$-\phi$	$-1-\phi$	−2	inactive
E_4	2	ϕ	$-1-\phi$	$-1-\phi$	ϕ	2	inactive

[a] $\phi = (\sqrt{5}-1)/2$. T_i for vibrational spectroscopy represents, with respect to the normal coordinate, dipole derivative component in the *i*-axis, and α_{ij} represents polarizability derivative tensorial component in the *i*- and *j*-axes.

In our previous study, a simpler 3/1 helix was assumed.[24] Although most of the observed spectra could be analyzed using a 3/1 helix, it is deemed necessary to obtain transmission spectra to observe detailed features for a more detailed analysis. Also, the 10/3 helix, and not the 3/1 helix, is the correct structure as found through X-ray analysis.[13,26] A 10/3 single helix analysis was therefore necessary before conducting a full trichroic crystal analysis. The vibrations of a correct helical symmetry should be established before analysis pertaining to frequency splittings for the crystal. The transmission infrared spectra, shown in Figure 4, obtained for an oriented electrospun fiber mat are the first reported instance of polarized transmission infrared spectra of oriented PLA α-crystals. In this and all spectra presented in this work, baseline correction was deemed unnecessary, and ordinate offsets were used to aid clarity. Generally good agreement with previous ATR results was achieved.

The character table for the line group C_{10}, shown in Table 1, would apply to analysis of polarized infrared spectra in Figure 4 that assumes a 10/3 helix for the α-crystal. C_{10} groups have three optically active symmetry species: A, E_1, and E_2. All three are Raman-active, of which only A and E_1 are infrared-active. In this case, bands more intense in the parallel infrared spectrum (that is, beam polarization is parallel to the oriented axis) belong to the A species; those in the perpendicular spectrum belong to the E_1 species. This oriented film analysis leads to results shown in the two columns to the left in Table 2. We note that in the carbonyl stretching band frequencies are observed that differ from those in a previous ATR-infrared study.[24] ATR is known to shift the peak frequency somewhat.[37] Peak frequencies obtained from the transmission mode are consistent with Raman spectroscopic observations.

To complete our previous normal-coordinate analysis on the PLA α-crystal,[24] we performed vibrational calculations on a 3/1 and a 10/3 helix. The results are tabulated in Table 3. Atomic coordinates corresponding to the graphics displayed in Figure 1 were used. As seen in the character tables of the C_{10} line group in Table 1 and C_3 line group,[32] the 3/1 helix with A and E and the 10/3 helix with A and E_1 species have the same number of infrared-active normal modes, since E_2 species are only Raman-active. We find that the bands below 900 cm^{-1} in particular are better reproduced by the simulated 10/3 helix spectrum. In some cases, for example the 411 and 397 cm^{-1} or the A species at 737 and 711 cm^{-1}, agreement between the 10/3 helix calculation and experimental data is far superior to the 3/1 helix calculation. The normal-coordinate calculation thus supports the 10/3 helical structure based on X-ray studies.[13,26] However, the complexity of the vibrational spectra observed, such as the three Raman bands or five infrared bands in the

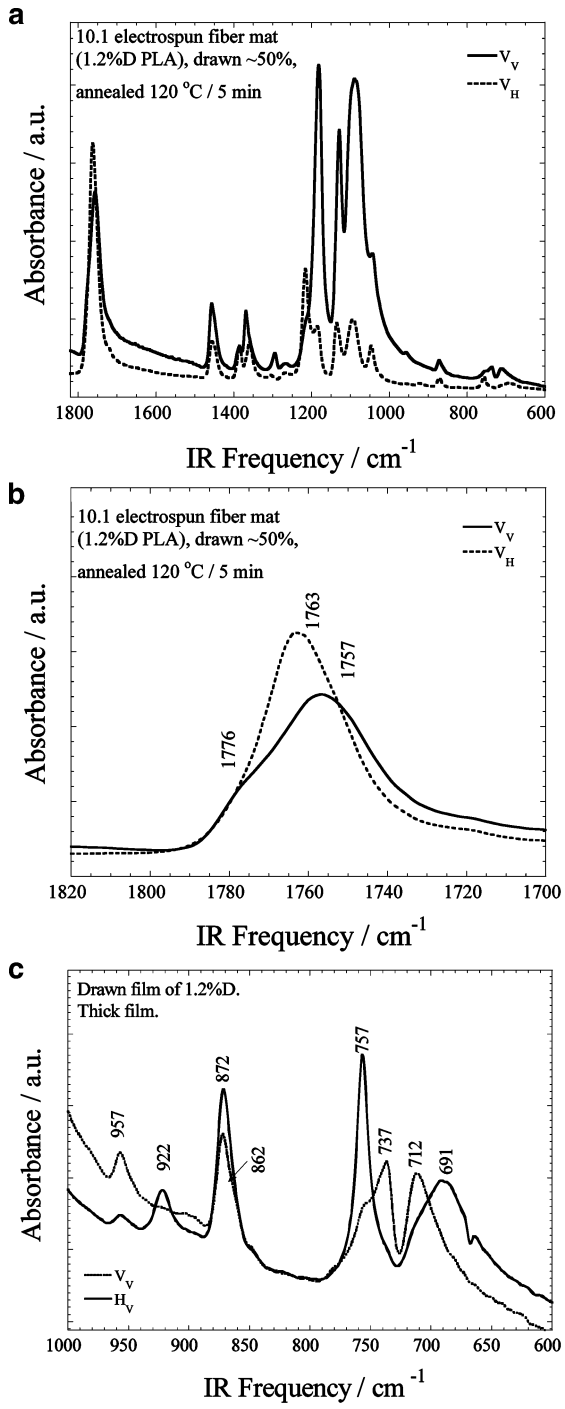

Figure 4. Polarized infrared spectra of PLA 1.2% D, electrospun into fiber mats from solution of DMF/chloroform mixture: (a) entire spectrum; (b) carbonyl stretch region; (c) backbone stretch region. V_V refers to the parallel spectrum and V_H to the perpendicular spectrum.

carbonyl stretch region for crystalline PLA, cannot be explained by the 10/3 helical structure alone. It is then concluded that a crystal group analysis must be conducted to explain fully the spectral features present in the α-crystal.

The point group of an α-crystal is D_2, with two helices in the unit cell. There are four symmetry species to D_2: A, B_1, B_2, and B_3. All species are Raman-active, and the B_i species are all infrared-active. According to the correlation table shown in Table 4, the E_1 species correlate in the same manner with the B_2 and B_3 species. That is, any E_1 vibration in the 10/3 helix will couple with the same E_1 vibration in the other 10/3 helix inside the *a*-crystal unit cell. The E_1 vibration of the two

Table 2. Group Symmetry Species Assignment to PLA α-Crystal Vibrations, from Polarized Infrared Spectra on Oriented Films and 2D Spherulites

C_{10}, A polarzd	C_{10}, E_1 depolarzd	D_2, A polarzd	D_2, B_1 depolarzd	D_2, B_2 depolarzd	D_2, B_3 depolarzd
				3006	3015
2997	2996	2997		2999	2997
				2965	
2945	2946	2947		2947	2947
		2882			2883
1776		1775	1777		1769
1757	1763	1764		1763	1759
				1750	1750
1457	1456		1457		1456
				1447	1443
1385	1386			1387	1387
				1382	
			1371		
	1359			1360	1360
1369	1305			1303	1306
			1293		1294
1294	1266			1223	1214
1267	1216			1212	1207
1185		1181		1201	
1182					1141
	1135			1136	1135
1129		1128		1108	
	1094		1090		1094
1090				1054	
	1047	1042		1047	1045
1044	923		958		
958				922	921
872	872	874	872	872	873
	757			757	754
		736	736		
737		711	712		
712				697	
	691				696
					688
		412			
		401			
		439			
		299			
		205			
		166			
		158			

helices in-phase and out-of-phase correspond to the B_2 and B_3 species. In the same manner, both the A and E_2 species in the C_{10} line group correlate to the A and B_1 species in the D_2 space group. Upon examination, we find that the B_1 species in D_2 correlate directly and uniquely with the A species in C_{10}, if only infrared-active vibrations are considered. On the basis of polarized infrared spectra on *c*-axis oriented PLA, specifically the oriented mats, B_1 species can be unambiguously assigned to bands that show greater intensity in the parallel as opposed to the perpendicular infrared spectrum.

For any uniaxially oriented sample examined under polarized light, only one axis (the orientation direction) is unique. The other two axes (perpendicular to the orientation direction) become indistinguishable due to cylindrical symmetry. Although our samples have only 60−70% crystallinity as measured by calorimetry, the polarized infrared data are of the highest quality available for PLA and clearly show features that could not be seen previously that belong to the α-crystal. Generally speaking, the accounting of spectroscopic features assignable to the amorphous phase in polymers is difficult. That is not the case here. It is known that these specific, well-defined vibrational splittings are very sensitive to the magnitude and specificity of the secondary interactions present. Usually the spectral features, both infrared and Raman, associated with the amorphous are quite diffuse and difficult to observe above the background. Therefore, all the sharp features observed in our spectra in this

Table 3. Calculated Frequencies from Normal-Coordinate Analysis for the 3/1 and 10/3 Helices and Experimental Frequencies from from Polarized Infrared Spectra on an Oriented Film[a]

3/1 helix		10/3 helix			experimental	
A	E	A	E_1	E_2	parallel	perpendicular
2961	2961	2961	2961	2961	2997	2996
2960	2960	2960	2960	2960	2945	2946
2935	2935	2936	2936	2935	1776	1763
2882	2882	2882	2882	2882	1757	1456
1771	1772	1766	1767	1768	1457	1386
1459	1459	1459	1459	1459	1385	1359
1457	1457	1457	1457	1457	1369	1305
1388	1383	1411	1403	1400	1294	1266
1376	1375	1383	1384	1385	1267	1216
1282	1272	1293	1288	1288	1185	1135
1191	1164	1183	1156	1147	1182	1094
1141	1120	1126	1115	1108	1129	1047
1082	1090	1074	1080	1077	1090	923
1032	1027	1029	1027	1027	1044	872
962	931	961	931	905	958	757
894	860	882	864	852	872	691
742	755	736	745	759	737	
690	698	705	701	710	712	
415	588	412	566	628		
354	404	363	397	388		
303	337	297	310	330		
241	229	230	226	231		
195	194	194	196	194		
148	160	157	168	165		
23	49	23	54	52		
	21		24	21		
				4		

[a] Polarized and depolarized Raman-active species are labeled accordingly.

Table 4. Correlation Table of the PLA Helix (C_{10}) Line to the α-Crystal (D_2)[a]

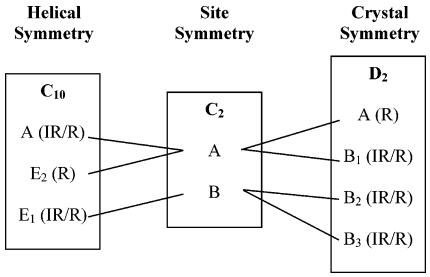

[a] "R" and "IR" refer to Raman and infrared activities, respectively.

study can be confidently assigned to the crystalline phase. In the case of 2D spherulites, we know from X-ray results (Figure 3) that the *a*-axis is the unique orientation axis. In this case, the bands more intense in the parallel spectrum belong to the B_3 species, as this species has a dipole derivative component purely in the *a*-axis direction of the crystal. In the case of oriented films, the *c*-axis is oriented, and the parallel spectrum shows stronger intensities for B_1 bands. In both *c*-axis and *a*-axis oriented samples, the B_2 species in the D_2 group is a perpendicular band. Bands not parallel in either the oriented mat sample or the spherulite sample belong by logical deduction to the B_2 species. In this manner, the symmetry species of all infrared-active bands of the α-crystal can be conclusively assigned. These assignments are summarized in the three columns to the right in Table 2.

The carbonyl stretching region is normally a region with only one band in the absence of strong interactions such as hydrogen bonding. If there are multiple bands in the region, then owing to the large dipoles of the C═O bond, there is the possibility of dipole−dipole interaction being the relevant intermolecular force. PLA shows splittings in infrared and Raman spectra in this region that require careful consideration. Quantitative explanation of data can provide valuable validation to the structural parameters used in our calculations. Infrared absorbance can be directly calculated with knowledge of the dipole derivative of a normal vibration.[38] The B_1 species of the carbonyl vibration was calculated to have a significantly lower absorbance than the B_2 or B_3 species in the infrared spectrum. The calculations were based on results from an ab initio calculation on a model compound, 2-methoxymethylpropanoate.[39] The dipole derivative of the carbonyl stretching vibration was extracted from the vibrational calculation. The dipole derivative was then directly transferred with respect to the O═C−O atoms and mapped onto the PLA α-crystal. The ab initio calculations found the dipole derivative value to be (−2.07, 0.13, 0.73) D/Å. The carbonyl carbon is set as the coordinate origin, the *x*-axis lying coincident with the C═O bond and the *y*-axis lying in the plane of the O═C−O bond angle. As vibrational amplitudes of each C═O in the α-crystal unit cell for each vibrational symmetry species (B_1, B_2, and B_3) are known from the D_2 character table, the α-crystal dipole derivative of the carbonyl stretching vibration for B_1, B_2, and B_3 can be computed. The result is shown in Table 5.

Table 5. Predicted Infrared Intensity of the 10/3 Helix and the α-Crystal Based on ab Initio Calculation on a Model Compound

C_{10}	relative IR intensity	D_2	relative IR intensity
A	0.13	A	0.00
E_1	1.00	B_1	0.13
E_2	0.00	B_2	0.34
		B_3	0.66

Carbonyls usually undergo a significant change in dipole moment for the corresponding vibrations, so that infrared absorbance is intense for their vibrations. However, Raman scattering also has considerable intensity for the carbonyl stretching vibration that is split into three components. The A species of the D_2 group shows a polarized Raman band. With polarized and depolarized Raman spectra for a 3D spherulite of the α-crystal, as shown in Figure 5, assignment of the A symmetry species becomes possible. The isotropic Raman spectra, where only A symmetry species have nonzero intensities, was calculated. In this case, the B_1, B_2, and B_3 species cannot be distinguished, since the B_i species are all depolarized, and the crystals are randomly oriented. The A species assignment for the α-crystal from Raman is reported in Table 2. We find that the bands visible in the carbonyl stretching region are in fact all polarized bands and thus have A symmetry. Analyses

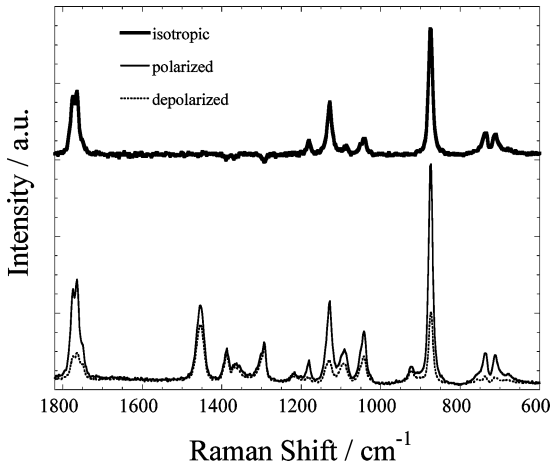

Figure 5. Polarized Raman spectra of 3D spherulite of PLA 1.2% D α-crystal.

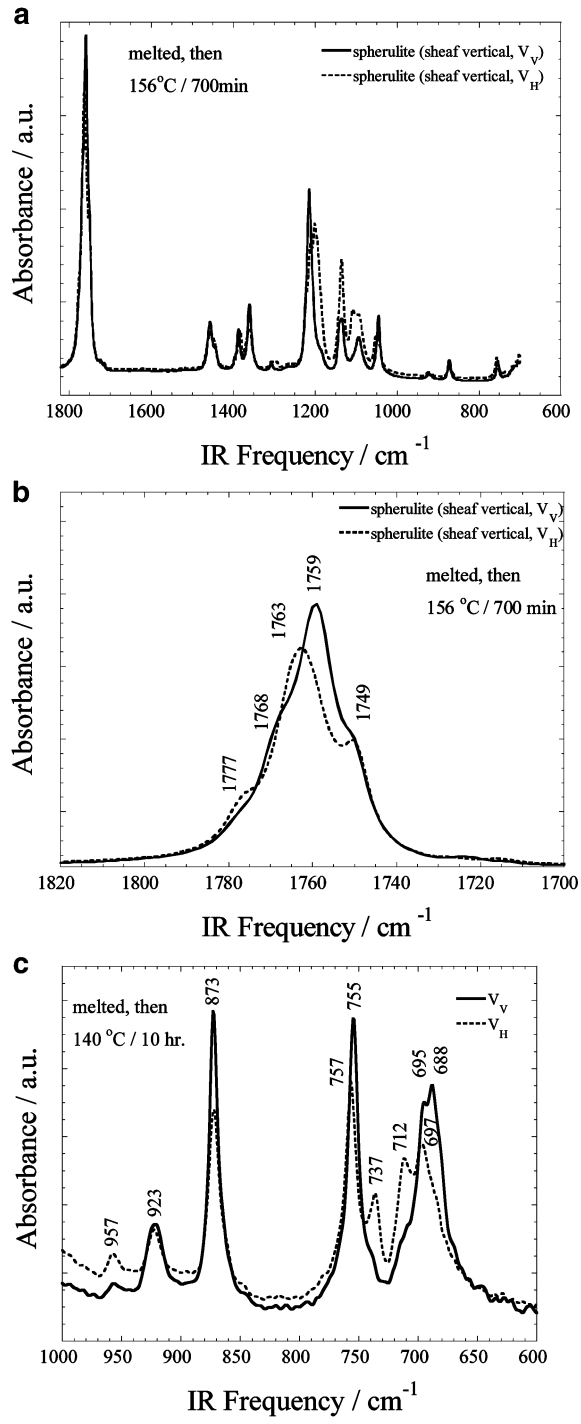

Figure 6. Polarized infrared spectra of PLA 2D spherulite: (a) entire spectrum; (b) carbonyl stretch region; (c) backbone stretch region. V_V refers to the parallel spectrum and V_H to the perpendicular spectrum.

of the spectra obtained for oriented film and spherulites are summarized in Table 3. More overlapped vibrations can be found. For example, in Figure 8, the polarized Raman spectra of amorphous PLA seem to suggest that the band at 1756 cm^{-1} is an E_1 species and that at 1763 cm^{-1} is an A species. The polarized infrared spectra in Figure 4 for *c*-axis-oriented PLA, however, show that the infrared band at 1757 cm^{-1} is A and that at 1763 cm^{-1} is E_1. To reconcile these results, we conclude that there are many overlapped carbonyl stretching bands for the α-crystal that can only be distinguished through use of both infrared and Raman spectroscopy.

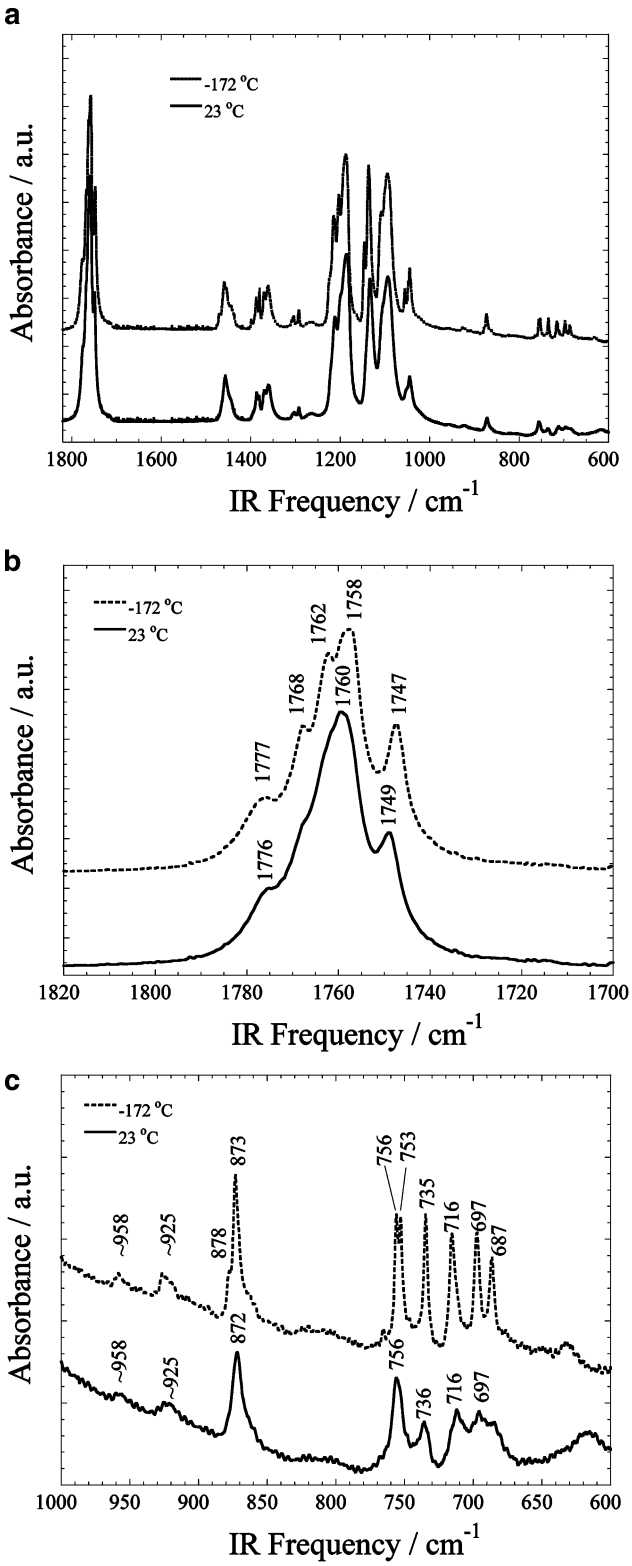

Figure 7. Cryogenic infrared spectra of PLA 1.2% D spherulite, prepared by melt-quenching and then crystallizing at 156 °C for 700 min: (a) entire spectrum; (b) carbonyl stretch region; (c) backbone stretch region. V_V refers to the parallel spectrum and V_H to the perpendicular spectrum.

In addition, we find that spherulitic, α-crystalline samples show many more band splittings, as shown in Figure 6, which were small in magnitude and did not appear in the drawn fiber mat infrared dichroism analysis given in Figure 4. These splittings do not exist in the amorphous state and furthermore exhibit polarized infrared absorption characteristics consistent

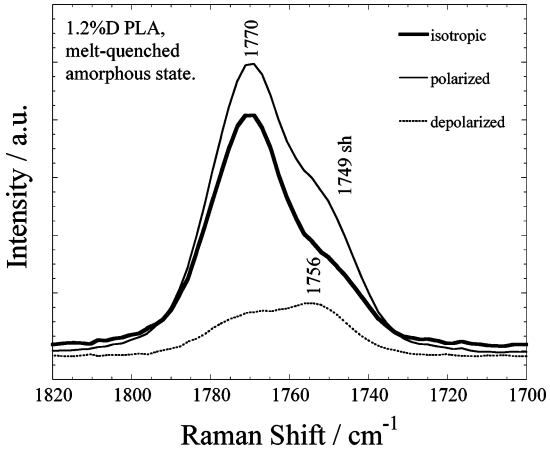

Figure 8. Polarized Raman spectra of PLA 1.2% D melt-quenched pellet.

Table 6. List of Internal Coordinate Symbols Used

symbol	corresponding internal coordinate
S	C═O stretch
R_1	C_α−C stretch
R_2	O−C_α stretch
R_3	C−O stretch
R	C_α−C_β stretch
Ω	C═O deformation
ω	skeletal C−O−C_α bend
α	CH_3 asymmetric bend
β	CH_3 rocking
δ_1	CH_3 side chain bend
δ_2	CH_3 side chain bend
δ_3	skeletal C−C_α−O bend
θ	C═O in-plane bend

with correlation splitting; for example, the 757 and 755 cm^{-1} bands can be assigned respectively to the B_2 and B_3 species of the D_2 space group. Therefore, the splittings are attributed to crystal field splitting.[22,23]

Crystal field splitting occurs due to the presence of more than one equivalent asymmetric species in the unit cell that interact, thus changing the energies of the vibrational states which without interaction would be degenerate in energy. The correlation table in Table 4 illustrates this fact. Therefore, in infrared, if interchain interaction is significant, A species of the C_{10} group (α-crystal) can split into A and B_1, and E_1 species can split in the same manner into B_2 and B_3, in the α-crystal. A cryogenic infrared spectrum of the PLA α-crystal in Figure 7 further demonstrates that under conditions where the unit cell volume would be reduced and interatomic distances would decrease, previously unseen band splittings emerge. Bands that were only shoulders in polarized infrared spectra have clearly distinguishable peaks under cryogenic conditions. Shorter interatomic distances usually translate into enhanced interactions. Therefore, the cryogenic spectra are further evidence that intermolecular interactions are the origins to band splittings.

Regarding vibrational activity analysis, it is important to note that PLA chain symmetry is higher as a single helix than its site symmetry in the crystal. The PLA α-helix possesses C_{10} symmetry. As it crystallizes into its orthorhombic form, PLA chain site symmetry with respect to the entire crystal is only C_2. Therefore, five degenerate vibrations each for B_1, B_2, and B_3 due to the loss of symmetry (the totally symmetric A vibration is not affected) are to be expected. For each species, crystal field can split these degenerate vibrations into separate components. This is consistent with the fact that there are multiple numbers of both B_2 and B_3 bands present in the carbonyl stretch region (see Table 2).

A complete discussion on band splitting in the carbonyl stretching region requires that Fermi resonance be considered. As seen in Figure 8, the carbonyl stretching region shows 1750 and 1770 cm^{-1} shoulders, both of which are polarized bands and therefore belong to the A symmetry species. These bands have been observed to exist for all amorphous PLA samples. In addition, the 1750 cm^{-1} shoulder is observed to sharpen, gain in intensity, and progress into a separated peak as the amorphous PLA crystallizes. This implies that the 1750 cm^{-1} shoulder is associated with the PLA crystalline conformation, *tg′t*. The 1770 cm^{-1} band, as it splits into two bands from crystal field splitting effects, is clearly associated with the helical *tg′t* conformation. [24] Both bands can be associated with crystalline PLA which exists only in one helical conformation for homochiral chains. The contention that the 1750 and 1770 cm^{-1} bands represent differences in chiral unit enchainment of PLA in the amorphous state [15] can then be rejected, since it is inconsistent with our data. These two bands may instead arise from Fermi resonance. The phenomenon is described as a spectral band splitting phenomenon due to accidental degeneracy of a fundamental and a higher ordered vibrational transition.[40] For such resonance to occur, the overtone or combination tone must have the same symmetry as the fundamental tone in question. In addition, there must be mechanical coupling between the overtone or combination and the fundamental vibrational modes; that is, the two vibrational levels involved must have nonzero displacement in the same internal coordinate. Those possible are listed in Table 6. Finally, the vibrational energies of the two levels must match closely. The smaller the energy difference, the the stronger resonance and therefore the larger splitting and redistribution in spectral intensity.[40,41] On the basis of these criteria, candidates for overtones or combination tones in Fermi resonance with the fundamental carbonyl stretching tone are identified and listed in Table 7. The fundamental carbonyl stretching vibration has the following internal coordinates to be active: S, Ω, R_3. Since the overtone of 873 cm^{-1} (both A and E) involves R_3 and Ω internal coordinates, as the carbonyl stretching mode, it is a strong candidate for being the vibrational transition in Fermi resonance with the carbonyl stretch. The combination of 1368 and 412 cm^{-1} is another viable candidate,

Table 7. Possible Candidates for Combinations or Overtones in Fermi Resonance with the Carbonyl Stretch Fundamental Tone Belonging to the A Symmetry Species[a]

possible combinations or overtones	potential energy distribution	symmetry of the fundamental(s)	symmetry of the combination or overtone	sum of harmonic frequencies
1368	R_3, θ, R_2, R_1	A × A	A	1780
412	δ_2, R_3, θ			
overtone of 873	R_1, β, ω, R_3, Ω	A	A	1746
overtone of 873	R_1, R, ω, R_3, Ω	E	A	1746
1356	R_3, θ, R_2, R_1	E × E	2A + E	1754
398	θ, δ_3, δ_2			
1455	α, β	A × A	A	1752
297	δ_1,δ_2,ω			

[a] The frequencies in question are from 3/1 helix normal-coordinate analysis.[24]

as both components of the combination tone involve the R_3 coordinate. The ability to affect the vibrations involved with the overtone or combination tone separately from the carbonyl would aid in identifying the actual overtone or combination tone in Fermi resonance with the carbonyl stretching vibration.

Conclusions

Highly oriented samples of PLA 2D spherulites and electrospun fiber mats were analyzed using polarized infrared spectroscopy. The results from those two infrared dichroism studies were combined to perform trichroic vibrational analysis. Correct Raman and infrared activities as well as an accurate character table for the C_{10} line group were derived. Correlation between the C_{10} helical vibrations and the D_2 orthorhombic crystal vibrations was established. Normal-coordinate analysis was conducted on the 10/3 and 3/1 helical structures. Simulated frequencies for the 10/3 helix reproduced the experimental peak frequencies better than those for the 3/1 helix, particularly in the lower, conformation-sensitive regions. This confirms that the 10/3 helix provides the better description of the PLA structure. Polarized infrared and Raman spectra led to unambiguous assignments of A, B_1, B_2, and B_3 crystal vibrations of the orthorhombic PLA α-crystal. Success of the α-crystal vibrational assignments validates the orthorhombic crystalline structure. This analytical method is expected to be generally applicable for semicrystalline polymer systems that have a trichroic crystalline polymorph and that exhibit spherulitic morphology. The numerous band splittings unobserved in our previous spectroscopic study that emerge in highly crystalline PLA are attributed to crystal field splitting affected by the presence of intermolecular interactions, i.e., carbonyl dipole interactions in the case of band splittings in the 1700−1850 cm^{-1} frequency range. In addition, both amorphous and crystalline PLA have what is interpreted as a Fermi resonance splitting in the carbonyl stretching frequency. Examination of vibrational symmetry and potential energy distribution indicated that the overtone of the 873 cm^{-1} band or the combination tone of the 1368 and 412 cm^{-1} bands are the most likely higher ordered vibrations that are in Fermi resonance with the carbonyl stretching fundamental vibration.

Acknowledgment. The authors thank the National Science Foundation-Environmental Protection Agency (TSE Grant RD831636010) and the New England Green Chemistry Consortium for the financial support of this project. In addition, a grant from Bioabsorbable Vascular Solutions, a subsidiary of Guidant, is greatly appreciated. K.A. thanks Dr. Sian Fennessey for technical and theoretical guidance in using the electrospinning facility and Professor Howard D. Stidham for extensive discussions on group analysis on crystals.

References and Notes

(1) Manome, A.; Okada, S.; Uchimura, T.; Komagata, K. *J. Gen. Appl. Microbiol.* **1998**, *44*, 371−374.
(2) Baratian, S.; Hall, E. S.; Lin, J. S.; Xu, R.; Runt, J. *Macromolecules* **2001**, *34*, 4857−4864.
(3) Takasaki, M.; Ito, H.; Kikutani, T. *J. Macromol. Sci., Phys.* **2003**, *B42*, 57−73.
(4) Celli, A.; Scandola, M. *Polymer* **1992**, *33*, 2699−2703.
(5) Liao, K. R.; Quan, D. P.; Lu, Z. J. *Eur. Polym. J.* **2002**, *38*, 157−162.
(6) Jain, R.; Shah, N. H.; Malick, A. W.; Rhodes, C. T. *Drug Dev. Ind. Pharm.* **1998**, *24*, 703−727.
(7) Jain, R. A. *Biomaterials* **2000**, *21*, 2475−2490.
(8) Hedrick, J. L.; Carter, K. R.; Labadie, J. W.; Miller, R. D.; Volksen, W.; Hawker, C. J.; Yoon, D. Y.; Russell, T. P.; McGrath, J. E.; Briber, R. M. In *Progress in Polyimide Chemistry I*; 1999; Vol. 141, pp 1−43.
(9) Smith, P. B.; Leugers, A.; Kang, S.; Yang, X.; Hsu, S. L. *Macromol. Symp.* **2001**, *175*, 81−94.
(10) Smith, P. B.; Leugers, A.; Kang, S.; Hsu, S. L.; Yang, X. *J. Appl. Polym. Sci* **2001**, *82*, 2497−2505.
(11) Yang, X.; Kang, S.; Yang, Y.; Aou, K.; Hsu, S. L. *Polymer* **2004**, *45*, 4241−4248.
(12) Sasaki, S.; Asakura, T. *Macromolecules* **2003**, *36*, 8385−8390.
(13) Aleman, C.; Lotz, B.; Puiggali, J. *Macromolecules* **2001**, *34*, 4795−4801.
(14) Zhang, J. M.; Tsuji, H.; Noda, I.; Ozaki, Y. *Macromolecules* **2004**, *37*, 6433−6439.
(15) Kister, G.; Cassanas, G.; Vert, M. *Polymer* **1998**, *39*, 267−273.
(16) Higgs, P. W. *Proc. R. Soc. London, Ser. A* **1953**, *220*, 472−485.
(17) Tadokoro, H. *J. Chem. Phys.* **1960**, *33*, 1558−1567.
(18) Turrell, G. In *Infrared and Raman Spectra of Crystals*; Academic Press: New York, 1972; pp 262−266.
(19) Smith, P. B.; Leugers, A.; Kang, S. H.; Hsu, S. L.; Yang, X. Z. *J. Appl. Polym. Sci.* **2001**, *82*, 2497−2505.
(20) Aou, K.; Kang, S.; Hsu, S. L. *Macromolecules* **2005**, *38*, 7730−7735.
(21) Schachtschneider, J. H.; Snyder, R. G. *Spectrochim. Acta* **1963**, *19*, 117−168.
(22) Snyder, R. G. *J. Mol. Spectrosc.* **1961**, *7*, 116−144.
(23) Tasumi, M.; Shimanou. T. *J. Chem. Phys.* **1965**, *43*, 1245−1258.
(24) Kang, S.; Hsu, S. L.; Stidham, H. D.; Smith, P. B.; Leugers, M. A.; Yang, X. *Macromolecules* **2001**, *34*, 4542−4548.
(25) Gazzano, M.; Focarete, M. L.; Riekel, C.; Scandola, M. *Biomacromolecules* **2004**, *5*, 553−558.
(26) De Santis, P.; Kovacs, A. J. *Biopolymers* **1968**, *6*, 299−306.
(27) Yang, X.; Kang, S.; Hsu, S. L.; Stidham, H. D.; Smith, P. B.; Leugers, A. *Macromolecules* **2001**, *34*, 5037−5041.
(28) Hoogsteen, W.; Postema, A. R.; Pennings, A. J.; ten Brinke, G.; Zugenmaier, P. *Macromolecules* **1990**, *23*, 634−642.
(29) Sawai, D.; Takahashi, K.; Sasashige, A.; Kanamoto, T.; Hyon, S. H. *Macromolecules* **2003**, *36*, 3601−3605.
(30) Ikada, Y.; Jamshidi, K.; Tsuji, H.; Hyon, S. H. *Macromolecules* **1987**, *20*, 904−906.
(31) Cartier, L.; Okihara, T.; Ikada, Y.; Tsuji, H.; Puiggali, J.; Lotz, B. *Polymer* **2000**, *41*, 8909−8919.
(32) Wilson, E. B., Jr.; Decius, J. C.; Cross, P. C. *Molecular Vibrations: The Theory of Infrared and Raman Vibrational Spectra*; Dover Publications: New York, 1955.
(33) Fennessey, S. F.; Farris, R. J. *Polymer* **2004**, *45*, 4217−4225.
(34) Moore, W. H.; Krimm, S. *Biopolymers* **1976**, *15*, 2439−2464.
(35) Frisch, M. J.; Trucks, G. W.; Schlegel, H. B.; Scuseria, G. E.; Robb, M. A.; Cheeseman, J. R.; Zakrzewski, V. G.; Montgomery, J. A.; Stratmann, R. E.; Burant, J. C.; Dapprich, S.; Millam, J. M.; Daniels, A. D.; Kudin, K. N.; Strain, M. C.; Farkas, O.; Tomasi, J.; Barone, V.; Cossi, M.; Cammi, R.; Mennucci, B.; Pomelli, C.; Adamo, C.; Clifford, S.; Ochterski, J.; Petersson, G. A.; Ayala, P. Y.; Cui, Q.; Morokuma, K.; Malick, D. K.; Rabuck, A. D.; Raghavachari, K.; Foresman, J. B.; Cioslowski, J.; Ortiz, J. V.; Stefanov, B. B.; Liu, G.; Liashenko, A.; Piskorz, P.; Komaromi, I.; Gomperts, R.; Martin, R. L.; Fox, D. J.; Keith, T.; Al-Laham, M. A.; Peng, C. Y.; Nanayakkara, A.; Gonzalez, C.; Challacombe, M.; Gill, P. M. W.; Johnson, B. G.; Chen, W.; Wong, M. W.; Andres, J. L.; Head-Gordon, M.; Replogle, E. S.; Pople, J. A. Gaussian, Inc., Pittsburgh, PA, 1998.
(36) Kang, S.; Hsu, S. L.; Stidham, H. D.; Smith, P. B.; Leugers, A.; Yang, X. *Macromolecules* **2001**, *34*, 4542−4548.
(37) Harrick, N. J. *Internal Reflection Spectroscopy*; John Wiley & Sons: New York, 1967.
(38) Colthup, N. B.; Daly, L. H.; Wiberley, S. E. *Introduction to Infrared and Raman Spectroscopy*, 3rd ed.; Academic Press: Boston, 1990.
(39) Levine, I. N. *Quantum Chemistry*, 5th ed.; Prentice Hall: Upper Saddle River, NJ, 2000.
(40) Herzberg, G. In *Infrared and Raman Spectra of Polyatomic Molecules*; D. Van Nostrand Co.: Princeton, NJ, 1945; Vol. 2, pp 215−218.
(41) Nyquist, R. A.; Settineri, S. E. *Appl. Spectrosc.* **1990**, *44*, 1629−1632.

MA052058+